

Interactions between the Ankyrin Repeat-Containing Protein Akr1p and the Pheromone Response Pathway in *Saccharomyces cerevisiae*

LING-RONG KAO, JULIE PETERSON,[†] RUIRU JI,[‡] LAUREL BENDER, AND ALAN BENDER*

Department of Biology, Indiana University, Bloomington, Indiana 47405

Received 9 June 1995/Returned for modification 31 July 1995/Accepted 23 October 1995

Akr1p, which contains six ankyrin repeats, was identified during a screen for mutations that displayed synthetic lethality with a mutant allele of the bud emergence gene *BEM1*. Cells from which *AKR1* had been deleted were alive but misshapen at 30°C and inviable at 37°C. During a screen for mutants that required one or more copies of wild-type *AKR1* for survival at 30°C, we isolated mutations in *GPA1*, which encodes the G_{α} subunit of the pheromone receptor-coupled G protein. (The active subunit of this G protein is $G_{\beta\gamma}$, and G_{α} plays an inhibitory role in $G_{\beta\gamma}$ -mediated signal transduction.) *AKR1* could serve as a multicopy suppressor of the lethality caused by either loss of *GPA1* or overexpression of *STE4*, which encodes the G_{β} subunit of this G protein, suggesting that pheromone signaling is inhibited by overexpression of Akr1p. Mutations in *AKR1* displayed synthetic lethality with a weak allele of *GPA1* and led to increased expression of the pheromone-inducible gene *FUS1*, suggesting that Akr1p normally (and not just when overexpressed) inhibits signaling. In contrast, deletion of *BEM1* resulted in decreased expression of *FUS1*, suggesting that Bem1p normally facilitates pheromone signaling. During a screen for proteins that displayed two-hybrid interactions with Akr1p, we identified Ste4p, raising the possibility that an interaction between Akr1p and Ste4p contributes to proper regulation of the pheromone response pathway.

The binding of peptide mating pheromones to their G protein-coupled receptors in *Saccharomyces cerevisiae* leads to the activation of a mitogen-activated protein (MAP) kinase cascade that effects changes in gene expression, the formation of mating projections, and cell cycle arrest (38). At the top of this cascade is MAP kinase kinase kinase Ste20p (44), which binds to and can be activated by the GTP-bound (active) form of the Rho-type GTPase Cdc42p (37, 45) (Fig. 1). Both Cdc42p and Cdc24p, which is a guanine nucleotide exchange factor that promotes the binding of GTP by Cdc42p (46), are required for efficient pheromone signaling (37, 45).

It is not clear how $G_{\beta\gamma}$ contributes to the activation of Ste20p's kinase activity toward MAP kinase kinase Ste11p (44). One model is that $G_{\beta\gamma}$ stimulates the guanine nucleotide exchange factor activity of Cdc24p toward Cdc42p. This possibility is supported by the finding that Ste4p (G_{β}) displays a two-hybrid interaction with Cdc24p (45). However, although mutationally activated Cdc42p can bypass the need for Cdc24p in pheromone signaling, activation of Cdc42p is not sufficient to stimulate the pheromone response pathway in the absence of pheromone (37, 45). Thus, the manner by which $G_{\beta\gamma}$ promotes signal transduction must involve more than its possible role in the activation of Cdc42p.

A second possible role for $G_{\beta\gamma}$ is to promote the binding of Ste20p to Ste11p. Genetic, two-hybrid, and coimmunoprecipitation data suggest that Ste4p binds to Ste5p (43), which is a scaffolding protein that binds to Ste11p, the MAP kinase ki-

nase Ste7p, and the MAP kinases Fus3p and Kss1p (12, 30) (Fig. 1). By binding to both Cdc24p and Ste5p, $G_{\beta\gamma}$ could help bring Ste11p near to activated Cdc42p. If Ste20p is bound to Cdc42p, this could result in bringing together Ste20p and its target Ste11p.

It is also possible that $G_{\beta\gamma}$ plays a role in helping Cdc42p discriminate between its different potential targets, promoting the binding of Cdc42p specifically to Ste20p. Cla4p, a kinase that is similar in sequence to Ste20p and that can bind to GTP-bound Cdc42p, is a potential alternative target of Cdc42p (14). *CLA4* was identified during a screen for mutants that displayed synthetic lethality with mutations in *CLN1* and *CLN2*, which encode G_1 -type cyclins (15). It is thus likely that Cla4p acts in a process that is regulated by Cln1/Cln2-dependent kinase. Consistent with this view, deletion of *CLA4* leads to defects in cytokinesis, a process that begins during the assembly of the bud site, at the time in the cell cycle when Cln1/Cln2-dependent kinase is active (14).

There exists at least one other yeast kinase that was identified by the genome sequencing project (GenBank accession number Z48149), that is similar in sequence to Cla4p and Ste20p, and that is therefore a likely target of Cdc42p. This kinase ("Cla4-like" in Fig. 1) is more similar in sequence to Cla4p than to Ste20p and so is more likely to have functions that are similar to those of Cla4p than to those of Ste20p.

CDC42 and *CDC24* were originally identified on the basis of their roles in bud emergence (1, 18), a process that involves cell cycle-regulated rearrangements of cytoskeletal elements, including the assembly (or capture) of cortical actin patches at the presumptive bud site. Since there is as yet no evidence that Cla4p and Ste20p control the organization of actin, there may also exist other targets for Cdc42p (e.g., phospholipid kinases or actin-binding proteins) that mediate Cdc42p's effects on actin organization.

Although the functions of Ste20p appear to overlap with those of Cla4p, phenotypic analyses of *ste20* and *cla4* mutants

* Corresponding author. Mailing address: Department of Biology, Indiana University, Bloomington, IN 47405. Phone: (812) 855-0689. Fax: (812) 855-6705. Electronic mail address: abender@sunflower.bio.indiana.edu.

[†] Present address: The Blood Center of Southeastern Wisconsin, Milwaukee, WI 53201-2178.

[‡] Present address: Department of Biological Sciences, Purdue University, West Lafayette, IN 47907.

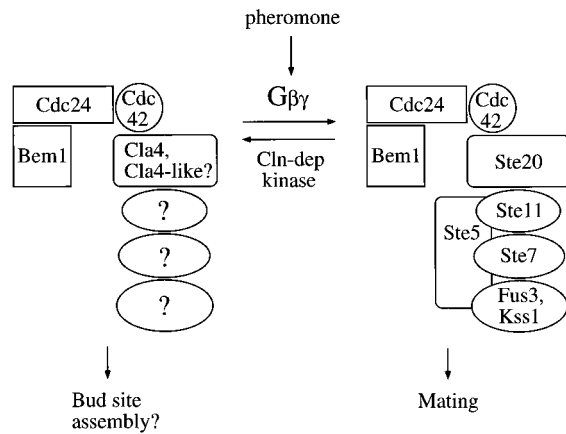


FIG. 1. Model in which $G_{\beta\gamma}$ and Cln-dependent kinase promote the formation of alternative Cdc42p-bearing signaling complexes. In this model, $G_{\beta\gamma}$ promotes the formation of a signaling complex containing Cdc24p and Ste20p, and Cln-dependent kinase promotes the formation of a signaling complex containing Cdc24p and Cla4p. A MAP kinase cascade that is different from the one involved in pheromone signaling is predicted to be regulated by Cla4p. Cla4-like is a kinase whose function might be similar to that of Cla4p.

suggest that Ste20p is principally involved in the pheromone response pathway and not in cytokinesis, whereas Cla4p is mainly required for cytokinesis and not for pheromone response (14, 22, 31). (It is not yet known whether Cla4p, like Ste20p [23], is involved in pseudohyphal development.) It thus seems likely that Cdc42p discriminates between Ste20p and Cla4p, activating Ste20p in response to the actions of $G_{\beta\gamma}$ and activating Cla4p in response to the actions of Cln-dependent kinase (Fig. 1).

SH3 domain-bearing protein Bem1p was discovered on the basis of its involvement in bud emergence (4, 9) and mating projection formation (10, 11). Both of these processes require asymmetric reorganizations of cortical actin patches and the localization of cell growth to a discrete region in the cell. Bem1p binds to Cdc24p (28) and so might play a role in the assembly of signaling and morphogenetic complexes containing Cdc24p and Cdc42p (Fig. 1). To learn more about the roles of Bem1p, we previously screened for mutations that displayed synthetic lethality with a mutant allele of *BEM1* (28). Four complementation groups of mutants that were also temperature sensitive (Ts^-) for viability were isolated. One group carried mutations in *CDC24*, supporting the view that the function of Bem1p is linked to that of Cdc24p. A second was mutant for *BEM2*, which encodes a GTPase-activating protein that can stimulate the GTPase activity of yeast Rho-type GTPase Rho1p (28). In the present study, we present evidence from genetic, phenotypic, and two-hybrid studies that *AKR1*, the third gene that was identified from the screen, is required for normal morphogenesis and inhibits pheromone signaling.

MATERIALS AND METHODS

Plasmids, strains, and media. The plasmids and strains used in this study are described in Tables 1 and 2. Plasmid pPB590, which contains *akr1-Δ1::URA3*, was made in multiple steps as follows. First, the 1.1-kb *HindIII-HindIII* fragment of DNA from pPB569 (Fig. 2), which contains sequences from the 3' end of *AKR1*, was inserted into the *HindIII* site of pBR322. Into the *Sall-PvuII* sites of the resulting plasmid was then inserted a 560-bp *Sall-PvuII* fragment of DNA bearing sequences from the 5' end of *AKR1* (from positions 184 to 0 in Fig. 2B). (In addition to containing the 184-bp *Sall-Sau3A* segment of *AKR1*, this 560-bp fragment also happened to contain an adjoining 190-bp *Sau3A-SphI* segment of the tetracycline resistance gene [from pPB569] fused to a 190-bp *SphI-PvuII* segment of M13mp19.) A 1.5-kb *BamHI-BamHI*, *URA3*-bearing fragment from *URA3-M13* (28) was then inserted into the *BamHI* site of the resulting plasmid

to give pPB590. In this plasmid, the segment of *AKR1* between codons 13 and 747 is replaced with *URA3*.

The media used in this study were YPD (1% yeast extract, 2% peptone, and 2% glucose), YPGalRaf (YPD with 3% galactose and 2% raffinose instead of glucose), SC (0.17% yeast nitrogen base without amino acids and ammonium sulfate, 0.5% ammonium sulfate, 2% glucose, 20 μ g of uracil per ml, 80 μ g of L-leucine per ml, 20 μ g of adenine sulfate per ml, 20 μ g of L-histidine per ml, 20 μ g of L-tryptophan per ml, 20 μ g of L-methionine per ml, and 30 μ g of L-lysine per ml), SC-Leu (SC without L-leucine), SC-Leu+Ade (SC-Leu containing 40 μ g of adenine sulfate per ml), SC-Trp-Leu (SC without L-tryptophan and L-leucine), SC-Trp-Leu+Ade (SC-Trp-Leu containing 40 μ g of adenine sulfate per ml), SC-Trp-Leu-His (SC-Trp-Leu without L-histidine), and SC-Ura (SC without uracil).

Microscopy. Cells were fixed in 5% formaldehyde and stained with 0.2 μ g of DAPI (4',6-diamidino-2-phenylindole) per ml in 1 mg of *p*-phenylenediamine per ml essentially as previously described (29). Cells were mounted under a coverslip and photographed with a Zeiss Axioplan fluorescence microscope using a 100 \times Plan-Neofluor oil immersion objective.

Screen for mutants that require one or more copies of *AKR1* for survival. Saturated cultures of strains PY655, PY657, PY658, and PY659 grown in SC-Leu were diluted in water and plated on YPD to give approximately 2,000 colonies per plate. Cells were mutagenized to 10% survival by UV irradiation. Plates were incubated at 30°C for 5 days and then stored at 4°C to allow the red color to develop. Uniformly red colonies were streaked twice on YPD to confirm that they displayed the mutant nonsectoring (*Sect^-*) phenotype. To check for recessiveness of the *Sect^-* phenotype, all PY655- and PY657-derived *Sect^-* mutants were crossed with Y388 (*MATa AKR1 ade2 ade3*) and all PY658- and PY659-derived *Sect^-* mutants were crossed with Y382 (*MATa AKR1 ade2 ade3*). Mating mixes were incubated for 1 day on YPD, diploids were then selected by streaking on SC-Trp-Lys, and cells from isolated colonies of the diploids were streaked on YPD to assay for sectoring. Each recessive mutant was transformed with *AKR1*-bearing plasmid pPB723 and control plasmid YEp24. Those mutants that became *Sect^+* when transformed with pPB723 and remained *Sect^-* when transformed with YEp24 were judged to require *AKR1* itself (as opposed to *ADE3* or *LEU2*) from pPB672 for survival.

Two-hybrid methodologies. The two-hybrid screen was performed with strain L40, which has the *HIS3* and *lacZ* reporter genes under the control of LexA. L40 containing plasmid pPB659 was transformed with a cDNA library fused to the transcriptional activation domain (AD) of *GAL4* (S. Elledge, Baylor College of Medicine). Transformants were selected on SC-Trp-Leu and then replicated to SC-Leu-Trp-His. *His^+* transformants were restreaked on SC-Trp-Leu plates. Colonies were imprinted onto Whatman 50 filter paper, frozen on dry ice, and incubated in Z buffer (60 mM Na_2HPO_4 , 40 mM NaH_2PO_4 , 10 mM KCl, 1 mM MgSO_4 , and 50 mM β -mercaptoethanol; pH 7.0) containing 0.3 mg of X-Gal (5-bromo-4-chloro-3-indolyl- β -D-galactopyranoside) per ml. Colonies were scored for the development of blue color 6 h after incubation at 30°C. Plasmids were recovered from the yeast cells and analyzed as previously described (28). A portion of each library insert adjacent to the AD was sequenced with primer TACCCTACAATGGATG.

Quantitative β -galactosidase activity assays. For the two-hybrid tests (see Table 6), cultures were grown at 30°C in SC-Trp-Leu+Ade. For the assays to determine the basal level of *pFUS1-lacZ* expression (see Table 7), cultures were grown at 24°C in SC-Leu+Ade (for plasmid-bearing strains Y1036 and Y1030) and SC-Ura (for plasmid-bearing strains Y1029 and Y1008). Cells from exponentially growing cultures were harvested at an optical density at 600 nm of between 0.2 and 0.6. All cultures were washed three times in Z buffer, and β -galactosidase activities were determined at 30°C as previously described (32).

The assays to measure the pheromone-induced levels of *pFUS1-lacZ* expression (see Table 8) were performed as described above, except for the following changes. Exponentially growing cultures of Y1056 carrying the indicated plasmids were grown in SC-Ura at 24°C to an optical density at 600 nm of between 0.3 and 0.5. α -Factor (Sigma Chemical Co., St. Louis, Mo.) was then added to a final concentration of 0.02 μ g/ml, and the cultures were incubated for an additional 4 h at 24°C.

Halo assays. A 0.4-ml portion of exponentially growing cultures at approximately 10^6 cells per ml was plated onto the appropriate selective medium (SC-Ura or SC-Leu). Sterile filter disks (diameter, 0.25 in. [0.635 cm]; Difco Laboratories, Detroit, Mich.) containing 15- μ l aliquots of α -factor at either 10 or 20 μ g/ml were then placed on the lawns, and the plates were incubated at 24°C for two days.

Nucleotide sequence accession number. The sequence of the *AKR1* locus was deposited in the GenBank database (accession number L31407).

RESULTS

Identification and molecular characterization of *AKR1*. We previously used an *ADE3/ade2 ade3*-based colony-sectoring assay to screen for mutants that required one or more copies of wild-type *BEM1* for survival at 30°C (28). The basis for the colony-sectoring assay is that *bem1 ade2 ade3* cells that carry

TABLE 1. Plasmids and phage used in this study

Plasmid or phage	Characteristic(s)
YCp50	<i>URA3 CEN4 ARS1</i> (25)
pPB569	<i>AKR1 URA3 CEN4 ARS1</i> (Fig. 2A). Isolated from a YCp50-based genomic library (33) on the basis of its ability to complement the Ts ⁻ growth defects of PY860.
pSL113	<i>LEU2</i> , 2 μ m ARS (5)
pPB575	<i>AKR1 LEU2</i> , 2 μ m ARS. Made by inserting a 6-kb <i>NruI</i> (from the tetracycline resistance gene)- <i>SpeI</i> (Fig. 2A) fragment from pPB569 into the <i>PvuII-XbaI</i> sites of pSL113.
pPB580	<i>AKR1 LEU2</i> , 2 μ m ARS. Made by inserting the 5-kb <i>SphI-SpeI</i> fragment from pPB569 (Fig. 2) into the <i>SphI-XbaI</i> sites of pSL113.
pPB665	<i>AKR1 URA3 CEN4 ARS1</i> (Fig. 2A). Isolated from a YCp50-based genomic library (33) by hybridization with a fragment of DNA from pPB569.
pPB590	<i>akr1-Δ1::URA3</i> (see Materials and Methods)
pPB672	<i>AKR1 ADE3 LEU2</i> , 2 μ m ARS. Made by inserting a 4.4-kb <i>NheI</i> (from the tetracycline resistance gene)- <i>XhoI</i> (Fig. 2A), <i>AKR1</i> -bearing fragment from pPB665 plus a 5-kb <i>SalI-BamHI</i> fragment bearing <i>ADE3</i> (21) into the <i>XbaI-BamHI</i> sites of pSL113.
YE24	<i>URA3</i> , 2 μ m ARS (7)
pPB723	<i>AKR1 URA3</i> , 2 μ m ARS. Made by inserting the 4.4-kb <i>NheI</i> (from the tetracycline resistance gene)- <i>XhoI</i> (Fig. 2A), <i>AKR1</i> -bearing fragment from pPB665 into the <i>NheI-SalI</i> sites of YE24.
JP350	<i>AKR1</i> in M13mp18. Made by inserting a 3.1-kb <i>NruI</i> (from the tetracycline resistance gene)- <i>PstI</i> (Fig. 2B) fragment from pPB569 into the <i>PstI-HincII</i> sites of M13mp18 and then converting the second and third codons of <i>AKR1</i> to a <i>BamHI</i> site by site-directed mutagenesis with oligonucleotide GCACATTCTTAATTCGGGATCCATCAATTAGCTACTC.
pCTC52	DBD _{<i>lexA</i>} -lamin, <i>TRP1</i> , 2 μ m ARS. Contains the DBD of the bacterial <i>lexA</i> gene fused to human lamin C cDNA (11a).
pPB659	DBD _{<i>lexA</i>} - <i>AKR1</i> , <i>TRP1</i> , 2 μ m ARS. Made by inserting the 2.4-kb <i>BamHI-PstI</i> fragment from JP350 into the <i>BamHI-PstI</i> sites of a version of pBTM116 (2) in which the <i>EcoRI</i> site was filled in by using Klenow fragment.
pPB922	AD _{<i>GAL4</i>} - <i>STE4</i> , <i>LEU2</i> , 2 μ m ARS. Isolate from the pACT-based cDNA library (S. Elledge, Baylor College of Medicine). Contains the transcriptional AD of <i>GAL4</i> fused to the 25th codon of <i>STE4</i> .
pKB40.1	AD _{<i>GAL4</i>} - <i>STE4</i> , <i>LEU2</i> , 2 μ m ARS (13). Contains full-length <i>STE4</i> fused to the AD.
pACTII	AD _{<i>GAL4</i>} , <i>LEU2</i> , 2 μ m ARS (17)
pSL1580	<i>mfa2Δ::pFUS1-lacZ URA3</i> . Contains sequences upstream and downstream of <i>MFa2</i> flanking a fusion between the promoter of <i>FUS1</i> and <i>lacZ</i> on a <i>URA3</i> -bearing, integrative vector (J. Horecka and G. Sprague, University of Oregon).
pRS315	<i>LEU2 CEN6 ARSH4</i> (36)
pPB741	<i>AKR1 LEU2 CEN6 ARSH4</i> . Made by inserting a 4.4-kb <i>NheI</i> (from the tetracycline resistance gene)- <i>XhoI</i> (Fig. 2A) fragment from pPB665 into the <i>XbaI-XhoI</i> sites of pRS315.
pRS316	<i>URA3 CEN6 ARSH4</i> (36).
pCY361	<i>BEM1 URA3 CEN6 ARSH4</i> (10). Made by insertion of a 2.1-kb <i>SmaI-KpnI</i> fragment containing <i>BEM1</i> into the <i>SmaI-KpnI</i> sites of pRS316.

wild-type *BEM1* on an *ADE3*-bearing plasmid are red. However, when grown on nonselective (e.g., YPD) medium, such cells form colonies that contain white sectors (Sect⁺ phenotype) because of the propagation of cells that lost the plasmid. In contrast, mutants that are dependent upon *BEM1* for survival form uniformly red colonies that lack white sectors (Sect⁻ phenotype), because those cells that have lost the plasmid are inviable. For convenience, we chose to study only those Sect⁻ mutants that were Ts⁻ for survival at 37°C. On the basis of complementation analysis of the Ts⁻ growth phenotype, Sect⁻ mutants PY858, PY859, and PY860 were judged to be in the same complementation group (group III [28]).

From a low-copy-number genomic library based in YCp50 (33), we isolated a plasmid (pPB569) that could rescue both the Ts⁻ growth defect (at 37°C) and the Sect⁻ phenotype (at 30°C) of all group III mutants. The complementing region was localized by subcloning and then sequenced (Fig. 2). It contains a single large open reading frame (Fig. 2B) which we call *AKR1* (for ankyrin repeat containing) and whose inferred product contains six copies of the ankyrin repeat (Fig. 2B and 3A). Ankyrin repeats are 33-amino-acid-long sequences that are present in a diverse set of proteins (26), including proteins that play roles in the organization of the cortical cytoskeleton (e.g., ankyrin [24]), proteins that are involved in signal transduction (e.g., Notch [41] and Cactus [20]), and inhibitors of cyclin-dependent kinases (e.g., p16 [35] and Pho81p [34]). On the basis of hydropathy analysis, Akrlp has several potential membrane-spanning stretches, the first and most hydrophobic

of which is marked in Fig. 2B. Akrlp also contains a region with similarity to the inferred products of five open reading frames that were identified during genome-sequencing projects but about which little is known (Fig. 3B).

To investigate the function of *AKR1*, we deleted it from a/α strain Y246 by gene replacement with a 3.8-kb *ClaI-PvuII* (both sites from within pBR322 sequences), *akr1-Δ1::URA3*-bearing fragment of DNA from pPB590 (Materials and Methods). The success of the deletion in Ura⁺ transformant Y927 was confirmed by Southern analysis on chromosomal DNA from Y246, Y927, and each segregant from a tetrad derived from Y927 (data not shown). Ura⁺ (*akr1-Δ1::URA3*) segregants from Y927 were viable but somewhat misshapen at 25°C, and they became more misshapen and died at 37°C. Most of these cells were elongated and multinucleate and appeared to be defective in cytokinesis (Fig. 4).

Diploids formed by crossing various *akr1-Δ1::URA3* strains with group III mutants PY858, PY859, and PY860 were Ts⁻ for growth at 37°C (data not shown), supporting the view that each of the group III mutants is indeed defective in *AKR1* function.

Genetic interactions between *AKR1* and *GPAL1*. To identify proteins whose functions are linked to Akrlp, we screened for mutants that required one or more copies of wild-type *AKR1* for survival at 30°C. We employed the *ADE3/ade2 ade3*-based colony-sectoring assay described above, using *akr1-1 ade2 ade3* strains bearing wild-type copies of *AKR1* and *ADE3* on a high-copy-number plasmid (pPB672). In previous synthetic lethal

TABLE 2. Yeast strains used in this study

Strain	Genotype ^a	Source or reference ^b
378	<i>MATa leu2:(LEU2 pGAL-STE4) bar1Δ ura3 leu2 trp1 his2 ade1</i>	D. Stone
L40	<i>MATa lys2:(LYS2 Op_{lexA}-HIS3) ura3:(URA3 Op_{lexA}-lacZ) leu2 ade2 trp1 his3</i>	40
PY655	<i>[AKR1 ADE3 LEU2] MATα akr1-1 ura3 leu2 ade2 ade3 trp1</i>	(Segregant from PY858 × Y379) transformed with pPB672
PY657	<i>[AKR1 ADE3 LEU2] MATα akr1-1 ura3 leu2 ade2 ade3 trp1</i>	Segregant from PY655 × Y388
PY658	<i>[AKR1 ADE3 LEU2] MATa akr1-1 ura3 leu2 ade2 ade3 lys2</i>	Segregant from PY655 × Y388
PY659	<i>[AKR1 ADE3 LEU2] MATa akr1-1 ura3 leu2 ade2 ade3 lys2</i>	Segregant from PY655 × Y388
PY744	<i>[AKR1 ADE3 LEU2] MATa gpa1-744 akr1-1 ura3 leu2 ade2 ade3 lys2</i>	Sect ⁻ mutant derived from PY658
PY778	<i>[AKR1 ADE3 LEU2] MATα gpa1-778 akr1-1 ura3 leu2 ade2 ade3 trp1</i>	Sect ⁻ mutant derived from PY657
PY809	<i>[AKR1 ADE3 LEU2] MATa gpa1-778 ura3 leu2 ade2 ade3 lys2</i>	Sect ⁻ segregant from PY778 × Y388
PY810	<i>[AKR1 ADE3 LEU2] MATa gpa1-744 akr1-1 ura3 leu2 ade2 ade3 lys2</i>	Sect ⁻ segregant from PY744 × Y382
PY839	<i>[AKR1 ADE3 LEU2] MATa/MATα gpa1::URA3/GPA1 akr1-1/AKR1 ura3/ura3 leu2/leu2 ade2/ade2 ade3/ade3 trp1/TRP1 lys2/LYS2</i>	Same as for PY852
PY852	<i>[AKR1 ADE3 LEU2] MATa/MATα gpa1::URA3/gpa1-778 akr1-1/AKR1 ura3/ura3 leu2/leu2 ade2/ade2 ade3/ade3 trp1/TRP1 lys2/LYS2</i>	PY778 × Y382 made <i>gpa1::URA3</i> by gene replacement with plasmid pG1203 (27)
PY855	<i>[AKR1 ADE3 LEU2] MATa/MATα gpa1-778:(GPA1 URA3)/gpa1-778 akr1-1/AKR1 ura3/ura3 leu2/leu2 ade2/ade2 ade3/ade3 trp1/TRP1 lys2/LYS2</i>	PY778 × [PY809 containing a <i>GPA1-URA3</i> integrative plasmid (C. Boone) integrated at <i>gpa1-778</i>]
PY858	<i>[BEM1 ADE3] MATa bem1-3 akr1-1 ura3 leu2 ade2 ade3 trp1</i>	Sect ⁻ mutant derived from PY429 (28)
PY859	<i>[BEM1 ADE3] MATα bem1-3 akr1-2 ura3 leu2 ade2 ade3 lys2</i>	Sect ⁻ mutant derived from PY431 (28)
PY860	<i>[BEM1 ADE3] MATα bem1-3 akr1-3 ura3 leu2 ade2 ade3 lys2</i>	Same as for PY859
PY897	<i>[AKR1 ADE3 LEU2] MATa/MATα ste3::LEU2/ste3::LEU2 gpa1::URA3/GPA1 (akr1-1 or AKR1)/AKR1 ura3/ura3 leu2/leu2 ade2/ade2 ade3/ade3 trp1/TRP1 lys2/lys2</i>	Segregant from Y969 × [segregant from (Y969 transformed with pPB672)]
PY976	<i>[AKR1 ADE3 LEU2] MATa/MATα akr1-Δ1::ura3/AKR1 MFa2:(mfa2::pFUS1-lacZ URA3)/MFa2 ura3/ura3 leu2/leu2 ade2/ade2 ade3/ADE3 lys2/LYS2 his3/HIS3</i>	(Y975 × Y955) transformed with pPB672
PY977	<i>[AKR1 ADE3 LEU2] MATa/MATα akr1-Δ1::ura3/AKR1 MFa2:(mfa2::pFUS1-lacZ URA3)/MFa2 ura3/ura3 leu2/leu2 ade2/ade2 ade3/ade3 lys2/LYS2 his3/HIS3</i>	Y389 × segregant from PY976
PY1014	<i>[AKR1 ADE3 LEU2] MATα akr1-Δ1::URA3 ura3 leu2 ade2 ade3 lys2</i>	Segregant from PY977 reverted to Ura ⁺
PY1054	<i>[AKR1 ADE3 LEU2] MATa gpa1-744 akr1-Δ1::URA3 ura3 leu2 ade2 ade3 lys2</i>	Segregant from PY1014 × PY744
Y246	<i>MATa/MATα ura3/ura3 leu2/leu2 his3/HIS3</i>	3
Y379	<i>MATα ura3 leu2 ade2 ade3</i>	Constructed as for Y382
Y382	<i>MATα ura3 leu2 ade2 ade3 trp1</i>	4
Y388	<i>MATa ura3 leu2 ade2 ade3 lys2</i>	4
Y389	<i>MATa ura3 leu2 ade2 ade3</i>	Constructed as for Y382
Y906	<i>MATα MFa2:(mfa2::pFUS1-lacZ URA3) ura3 leu2 ade2 ade3 trp1</i>	Plasmid pSL1580 integrated into Y382
Y907	<i>MATα mfa2::pFUS1-lacZ ura3 leu2 ade2 ade3 trp1</i>	Y906 made Ura ⁻ on 5FOA
Y927	<i>MATa/MATα akr1-Δ1::URA3/AKR1 ura3/ura3 leu2/leu2 his3/HIS3</i>	Y246 made <i>akr1-Δ1::URA3</i> by gene replacement with pPB590
Y935	<i>MATa akr1-1 ura3 leu2 ade2 ade3 trp1</i>	Segregant from PY858 × Y379
Y955	<i>MATa MFa2:(mfa2::pFUS1-lacZ URA3) ura3 leu2 ade2 ade3 lys2</i>	Segregant from Y906 × (PY658 cured of plasmid)
Y957	<i>MATα gpa1-778:(GPA1 URA3) akr1-1 ura3 leu2 ade2 ade3 trp1</i>	Segregant from PY855
Y969	<i>MATa/MATα ste3::LEU2/STE3 gpa1::URA3/GPA1 akr1-1/AKR1 ura3/ura3 leu2/leu2 ade2/ade2 ade3/ade3 trp1/TRP1 lys2/LYS2</i>	PY839 cured of plasmid and made <i>ste3::LEU2</i> by gene replacement with pSL376 (16)
Y975	<i>MATα akr1-Δ1::ura3 ura3 leu2 his3</i>	(Segregant from Y927) made Ura ⁻ on 5FOA
Y994	<i>MATα gpa1-744 ura3 leu2 ade2 ade3 trp1</i>	Segregant from (PY744 × segregant from PY855)
Y1008	<i>MATα bem1::LEU2 mfa2::pFUS1-lacZ ura3 leu2 ade2 ade3</i>	Segregant from Y907 × PY899 (6)
Y1015	<i>MATa/MATα akr1-Δ1::ura3/akr1-Δ1::ura3 ura3/ura3 leu2/leu2 ade2/ade2 ade3/ade3 lys2/LYS2</i>	(Cross of two segregants from PY977) cured of plasmid
Y1026	<i>MATa akr1-Δ1::ura3 bar1-1 ura3 leu2 ade2</i>	Segregant from [(segregant from PY977) cured of plasmid × DJ211-5-3 (D. Jenness)]
Y1029	<i>MATa bem1::LEU2 mfa2::pFUS1-lacZ ura3 leu2 ade2 ade3 trp1 lys2</i>	Same as for Y1008
Y1030	<i>MATa akr1-Δ1::ura3 mfa2::pFUS1-lacZ ura3 leu2 ade2 ade3</i>	(Segregant from PY977) made Ura ⁻ on 5FOA
Y1031	<i>MATa bem1::LEU2 bar1-1 ura3 leu2 ade2 lys2 his4</i>	Segregant from [PY899 (6) × 7423-2-1 (J. Konopka)]
Y1036	<i>MATα akr1-Δ1::ura3 mfa2::pFUS1-lacZ ura3 leu2 ade2 ade3</i>	Same as for Y1030
Y1056	<i>MATa akr1-Δ1::ura3 mfa2::pFUS1-lacZ bar1::LEU2 ura3 leu2 ade2 ade3</i>	Y1030 made <i>bar1::LEU2</i> by gene replacement with plasmid pZV77 (V. MacKay)

^a Relevant markers on plasmids are indicated in brackets.

^b 5FOA, 5-fluoroorotic acid.

and multicopy suppressor screens that we have performed, different background mutations in our different starting strains have affected which mutants could be isolated (4, 25a). Therefore, we chose to use four different starting strains (PY655, PY657, PY658, and PY659) for the current screen. Thirty-eight recessive, *AKR1*-requiring Sect⁻ mutants were identified (Ma-

terials and Methods). Leakiness of the Sect⁻ phenotype made the analysis of many of these mutants difficult. However, because the Sect⁻ phenotype of isolates PY778 and PY744 was tight, we analyzed these mutants first.

Plasmids that could suppress the Sect⁻ phenotypes of a descendant of PY778 (strain PY809) and a descendant of

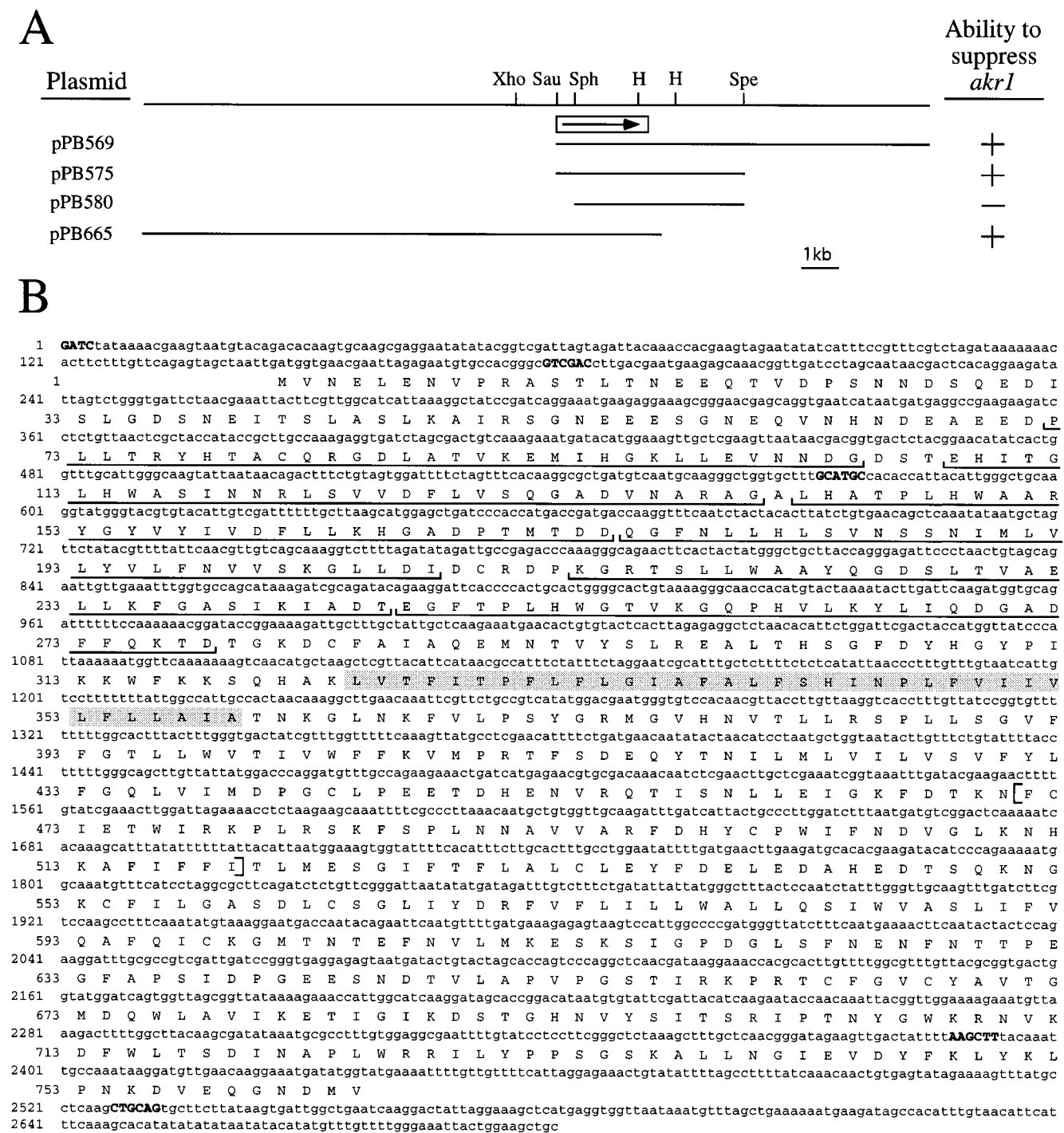


FIG. 2. Localization and sequence of *AKR1*. (A) The ability of plasmids containing the indicated segments of DNA to suppress the Ts^- growth defect of *akr1-1* mutant Y935 is shown. The box indicates the segment that was sequenced. The arrow shows the position of the *AKR1* open reading frame. Relevant *Xho*I (Xho), *Sau*3AI (Sau), *Sph*I (Sph), *Hind*III (H), and *Spe*I (Spe) sites are indicated. (B) Sequence of *AKR1* and the inferred Akr1 protein. The ankyrin repeats are indicated by underlining, the novel sequence motif (Fig. 3B) is marked with brackets, and the most hydrophobic stretch is shaded. All *Sal*I (179), *Sph*I (572), *Pst*I (2527), and relevant *Sau*3AI (1) and *Hind*III (2388) sites are capitalized in boldface type.

PY744 (strain PY810) were isolated from both low- and high-copy-number genomic libraries. On the basis of restriction and sequence analyses (data not shown), we deduced that each of these plasmids contained either *AKR1*, *MAT α* , or *GP1* (Table 3). *GP1* encodes the G_α subunit of the pheromone receptor-coupled G protein. Because $G_{\beta\gamma}$, when released from G_α ,

activates the pheromone response pathway, loss-of-function mutations in *GP1* result in permanent cell cycle arrest. Although loss of *GP1* function is lethal in haploids, it is not lethal in *MATa*/*MAT α* diploid cells because *MATa* and *MAT α* together repress the transcription of some of the genes that are required for pheromone signal transduction. On the basis of

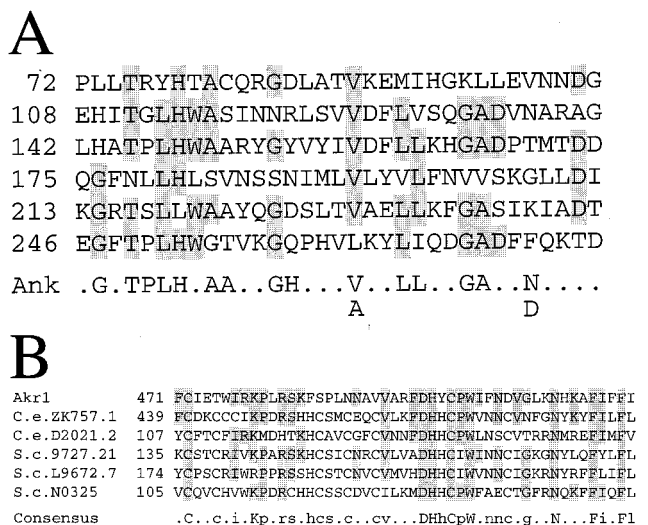


FIG. 3. Sequence alignments involving Akr1p. (A) Sequence alignment of the ankyrin repeats of Akr1p. The consensus sequence for the 23 ankyrin repeats in human erythrocyte ankyrin (24) is indicated below the six repeats in Akr1p. Identical amino acids within the ankyrin repeats of Akr1p are shaded. (B) Sequence alignment of a novel motif in Akr1p. The sequences for the following proteins are shown: *Caenorhabditis elegans* ZK757.1 gene product (Swiss-Prot no. P34679), *C. elegans* D2021.2 gene product (GenBank no. U23513), *S. cerevisiae* 9721.21 gene product (GenBank no. Z48758), *S. cerevisiae* L9672.7 gene product (GenBank no. U20865), and *S. cerevisiae* hypothetical protein N0325 (PIR no. S51289). Positions of identity with Akr1p are shaded. In the consensus sequence, capital letters correspond to positions in which all six sequences are identical and lowercase letters indicate positions in which at least four of the sequences are identical.

these considerations, we speculated that PY778 and PY744 were both defective in *GPA1* and that *MAT α* was isolated as a suppressor of *gpa1* because of the ability of *MAT α* , when in combination with endogenous *MAT α* (in PY809 and PY810), to prevent pheromone signaling.

The following analysis indicates that *AKR1* can indeed serve as a multicopy suppressor of *gpa1* and that the mutation responsible for the Sect⁻ phenotype of PY778 is tightly linked to *GPA1*. A null allele of *gpa1* (*gpa1::URA3*) was transplaced, by homologous recombination, into the diploid formed by crossing PY778 (putatively *gpa1*) and Y382 (*GPA1*). PCR analysis confirmed that the resulting Ura⁺ transformants PY852 and PY839 had become (heterozygously) *gpa1::URA3* (data not shown). All of the viable Ura⁺ (*gpa1::URA3*) segregants analyzed from PY852 and PY839 were Sect⁻ (Table 4), indicating that deletion of *GPA1* caused cells to require multiple copies of *AKR1* for survival. All of the Ura⁻ segregants analyzed from PY852 were Sect⁻, and all of the Ura⁻ segregants analyzed from PY839 were Sect⁺ (Table 4). The failure to recover Ura⁻ Sect⁺ recombinants from PY852 or Ura⁻ Sect⁻ recombinants from PY839 indicates that the mutation that is responsible for the Sect⁻ phenotype of PY778 is tightly linked to the *GPA1* locus. (We infer that, in PY839, *gpa1::URA3* recombined into the same chromosome [contributed by PY778] that contained the mutation responsible for the original Sect⁻ phenotype of PY778 and that, in PY852, *gpa1::URA3* recombined into the opposite chromosome.) In combination with the above findings that *GPA1* can suppress the Sect⁻ phenotype of PY778 and that *AKR1* can serve as a multicopy suppressor of a null allele of *gpa1*, these data strongly suggest that the mutation responsible for the Sect⁻ phenotype of PY778 is in *GPA1* itself.

In crosses between PY744 (*akr1-1*, putatively *gpa1*) and *AKR1 GPA1* strain Y382, tetrads in which all four segregants were viable but in which three or four of the segregants were Sect⁺ were isolated (data not shown), suggesting that PY744 may contain a partial-loss-of-function allele of *gpa1* that is not lethal by itself but which becomes lethal in an *akr1* mutant. Because the ability of *akr1* to display synthetic lethality with *gpa1* addresses the issue of whether Akr1p at normal dosage (and not just when overexpressed) can affect pheromone signaling, we explored this potential synthetic-lethal relationship further. In a cross between PY744 and an *akr1-1* strain containing a *URA3*-tagged copy of wild-type *GPA1* (strain Y957), all of the analyzed tetrads were of the parental ditype (Sect⁻ Ura⁻ or Sect⁺ Ura⁺ [Table 5]), indicating that the mutation responsible for the Sect⁻ phenotype is tightly linked to the *GPA1* locus. Combined with the previous finding that *GPA1* on a low-copy-number plasmid can suppress the Sect⁻ phenotype of PY744, these linkage data strongly suggest that PY744 does indeed contain a mutant allele of *GPA1*, which we call *gpa1-744*. In a cross between PY744 and *GPA1 akr1- Δ 1::URA3* strain PY1014, approximately half of the Sect⁻ segregants were Ura⁺ (Table 5), indicating that the Sect⁻ phenotype caused by *gpa1-744* is not dependent upon the particular mutant allele of *akr1* that was used in the synthetic-lethal screen.

To confirm that *gpa1-744* displays synthetic lethality with *akr1* (rather than that the *gpa1-744* mutation, by itself, causes cells to require multiple copies of *AKR1* for survival), we crossed *gpa1-744 akr1- Δ 1::URA3* strain PY1054 to both a *gpa1-744 AKR1* strain (Y994) and a *GPA1 AKR1* strain (Y382). As shown in Table 5, all of the *AKR1* (Ura⁻) segregants from both crosses were Sect⁺, indicating that the wild-type *AKR1* from the genome is sufficient to prevent *gpa1-744* mutants from requiring the *AKR1*-bearing plasmid for survival. All of the *akr1- Δ 1::URA3* segregants were Sect⁻ in the cross involving Y994 (in which all of the segregants were predicted to be *gpa1-744*), whereas only approximately half of the *akr1* segregants were Sect⁻ in the cross involving Y382 (in which only approximately half of all of the segregants were predicted to be *gpa1-744*), as predicted by the model in which *akr1- Δ 1::URA3* displays synthetic lethality with *gpa1-744*.

To investigate whether any of the other Sect⁻ mutants that were isolated in the screen for mutants that required one or more copies of *AKR1* for survival were defective in *GPA1* function, we investigated the ability of *GPA1*, borne on a low-copy-number plasmid, to suppress the Sect⁻ phenotype of the remaining 36 mutants. Both of the PY659-derived mutants, 1 of the 6 PY655-derived mutants, 5 of the remaining 8 PY657-derived mutants, and 15 of the remaining 20 PY658-derived mutants became Sect⁺ when transformed with the *GPA1*-bearing plasmid but not when transformed with an empty vector (data not shown), suggesting that most of the Sect⁻ mutants were indeed defective for *GPA1*. The analysis of the 13 remaining Sect⁻ mutants will be presented elsewhere.

Genetic and two-hybrid interactions between *AKR1* and *STE4*. To identify proteins that associate with Akr1p, we screened a yeast cDNA library for genes whose products displayed two-hybrid interactions with a DNA-binding domain of LexA (DBD)-Akr1p fusion (Materials and Methods). Nine clones that caused high levels of expression of a *lacZ* reporter gene when in combination with DBD-Akr1p but that gave no induction of *lacZ* when in combination with a control DBD fusion to human nuclear lamin were isolated. Sequence analysis revealed that three of the clones contained AD fusions to the 13th codon of *GCSI*, which encodes a putative Zn²⁺ finger-bearing protein implicated in the exit of cells from stationary phase (19); one contained a fusion to the C-terminal 47

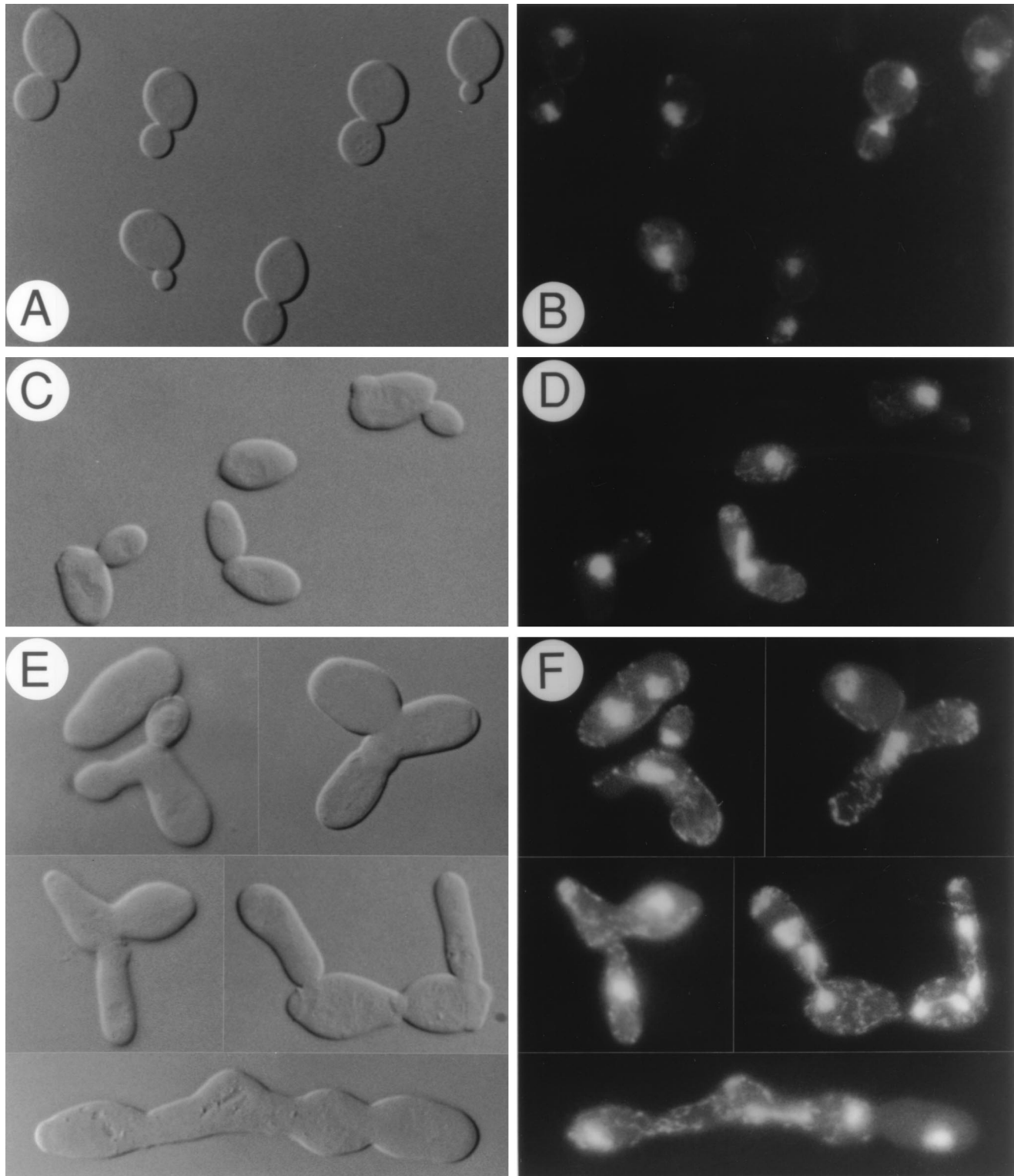


FIG. 4. Phenotypes of *akr1* mutants. Differential interference contrast (A, C, and E) and fluorescence (B, D, and F) images of cells from DAPI-stained *akr1* deletion strain Y1015 (C to F) and control strain PY977 cured of plasmid (A and B). Exponentially growing cultures were grown in YPD at 25°C (C and D) or were shifted from 25°C and grown at 37°C for 8 h (A, B, E, and F).

codons of the gene for 6-phosphogluconate dehydrogenase (GenBank accession no. U17155); and four contained open reading frames fused, in reverse orientation, to the AD (transcriptional AD of *GAL4*). These backward clones contained

the gene for ribosomal subunit L2 (twice), *GPM1* (encoding phosphoglycerate mutase), and a novel open reading frame.

Of greatest potential relevance to the present study was the finding that one of the library clones (plasmid pPB922) con-

TABLE 3. Genes isolated on the basis of their ability to suppress the Sect⁻ phenotype of PY809 and PY810

Strain	Gene	No. of isolates	
		YCp50 library ^a	YE24 library ^b
PY809	<i>AKR1</i>	0	1
	<i>MATα</i>	3	48
	<i>GPA1</i>	0	17
PY810	<i>AKR1</i>	7	3
	<i>MATα</i>	16	12
	<i>GPA1</i>	3	7

^a A low-copy-number genomic library (33).^b A high-copy-number genomic library (8).

tained an in-frame fusion to *STE4*, which encodes the G _{β} subunit of the pheromone receptor-coupled G protein. This fusion contained all but the first 24 codons of *STE4*. The DBD-Akr1p fusion could also display a two-hybrid interaction with an AD fusion to full-length *STE4* (Table 6), indicating that the interaction is not due to a special property of the truncated version of *STE4* that was isolated from the screen.

The finding that Akr1p can display a two-hybrid interaction with Ste4p raises the possibility that Akr1p inhibits pheromone signaling by blocking the binding of G _{$\beta\gamma$} to its target (or targets). Another possibility is that Akr1p itself is a target of G _{$\beta\gamma$} and that the binding of G _{$\beta\gamma$} to Akr1p inhibits the negative effects of Akr1p on pheromone signaling. Consistent with either general model, we found that *AKR1* could serve as a multicopy suppressor of the lethality that is caused by overexpression of *STE4* from a *GAL* promoter construct (Fig. 5).

We considered the possibility that if Akr1p inhibits G _{$\beta\gamma$} function, it might do so by inhibiting the release of G _{$\beta\gamma$} from the pheromone receptors. To investigate this possibility, we asked whether the α -factor receptor (Ste3p) is required in α cells for *AKR1* to serve as a multicopy suppressor of the lethality caused by loss of G _{α} . As shown in Table 4, viable *MAT α ste3::LEU2 gpa1::URA3* segregants, which were all Sect⁻, were readily obtained from *MAT α /MAT α ste3::LEU2/ste3::LEU2 gpa1::URA3/GPA1*, pPB672 (*AKR1*, *ADE3*, 2 μ m)-bearing strain PY897. Thus, pheromone receptor is not required for *AKR1* to serve as a multicopy suppressor of *gpa1*.

Sensitivity of *akr1* and *bem1* mutants to pheromone. To investigate further whether Akr1p normally inhibits the pheromone response pathway, we asked whether deletion of *AKR1* leads to increased expression of pheromone-inducible gene *FUS1*. The basal level of expression of *FUS1* is due to a con-

TABLE 4. Linkage analysis of *gpa1::URA3* and the mutation responsible for the Sect⁻ phenotype of PY778^a

Strain	No. of segregants				Inferred genotype
	Sect ⁻		Sect ⁺		
	Ura ⁺	Ura ⁻	Ura ⁺	Ura ⁻	
PY852 ^b	9	9	0	0	<i>gpa1-778/gpa1::URA3</i>
PY839 ^c	9	0	0	20	<i>gpa1::URA3/GPA1</i>
PY897	24 ^d	0	0	33	<i>ste3::LEU2/ste3::LEU2 gpa1::URA3/GPA1</i>

^a The sectoring phenotype was assayed at 30°C.^b Not included are two inviable segregants from the five tetrads that were analyzed. Both of these segregants were inferred to be Ura⁺.^c Not included are 11 inviable segregants from the 10 tetrads that were analyzed. All of these segregants were inferred to be Ura⁺.^d Thirteen of these were α .TABLE 5. Sectoring phenotype of segregants from crosses involving *gpa1-744* and *akr1*^a

Cross (relevant genotype)	No. of segregants			
	Sect ⁻		Sect ⁺	
	Ura ⁺	Ura ⁻	Ura ⁺	Ura ⁻
PY744 (<i>gpa1-744 akr1-1</i>) \times Y957 [<i>gpa1-778:(GPA1 URA3) akr1-1</i>] ^b	0	20	34	0
PY744 (<i>gpa1-744 akr1-1</i>) \times PY1014 (<i>GPA1 akr1-Δ1::URA3</i>) ^c	9	11	13	11
PY1054 (<i>gpa1-744 akr1-Δ1::URA3</i>) \times Y994 (<i>gpa1-744 AKR1</i>) ^d	19	0	0	43
PY1054 (<i>gpa1-744 akr1-Δ1::URA3</i>) \times Y382 (<i>GPA1 AKR1</i>) ^e	13	0	20	38

^a The sectoring phenotype was assayed at 30°C.^b Not included are 14 inviable segregants from the 17 tetrads that were analyzed. All of these segregants were inferred to be Ura⁻.^c Not included are four inviable segregants from the 12 tetrads that were analyzed. Two of these segregants were inferred to be Ura⁺, and two were inferred to be Ura⁻.^d Not included are 26 inviable segregants from the 22 tetrads that were analyzed. Twenty-five of these segregants were inferred to be Ura⁺, and one was inferred to be Ura⁻.^e Not included are 17 inviable segregants from the 22 tetrads that were analyzed. Ten of these segregants were inferred to be Ura⁺, and seven were inferred to be Ura⁻.

stitutive, low level of activity of the signaling pathway that is present even in the absence of pheromone (39). To assay *FUS1* expression, we measured the β -galactosidase activity of two *akr1- Δ 1::ura3* strains that carried an integrated version of a *pFUS1-lacZ* reporter construct. Such cells expressed three- to fourfold more β -galactosidase activity in the absence of *AKR1* than when *AKR1* was carried on a low-copy-number plasmid (Table 7, strains Y1030 and Y1036), supporting the view that *AKR1* normally inhibits pheromone signaling. Increasing the copy number of *AKR1* (with a high-copy-number plasmid) decreased further the basal level of expression of *pFUS1-lacZ*, as expected (Table 7). Although Akr1p clearly affects the basal level of *pFUS1-lacZ* expression, deletion of *AKR1* had no significant effect on the pheromone-induced level of *pFUS1-lacZ* (Table 8).

Given that *AKR1* was identified on the basis of a genetic interaction with *BEM1*, we were curious to know whether Bem1p also affects pheromone signaling. As shown in Table 7, cells from which *BEM1* had been deleted (strains Y1008 and Y1029) expressed approximately one-sixth the amount of *pFUS1-lacZ* as did the same cells carrying a wild-type copy of *BEM1* on a low-copy-number plasmid, suggesting that Bem1p

TABLE 6. Two-hybrid interaction between Akr1p and Ste4p^a

DBD	Protein		β -Galactosidase activity ^b
	AD ^c		
Lamin	—		0.07
Lamin	Ste4p		0.10
Akr1p	—		0.07
Akr1p	Ste4p		25

^a The proteins that are fused to the DBD and the transcriptional AD are indicated. Assays were performed with strain L40 bearing combinations of the following plasmids: pCTC52 (DBD-lamin), pPB659 (DBD-AKR1), pACTII (AD), and pKB40.1 (AD-STE4).^b β -Galactosidase activities are given as the average value from four independent transformants (see Materials and Methods). Each measured value was within 60% of the average.^c —, AD alone.

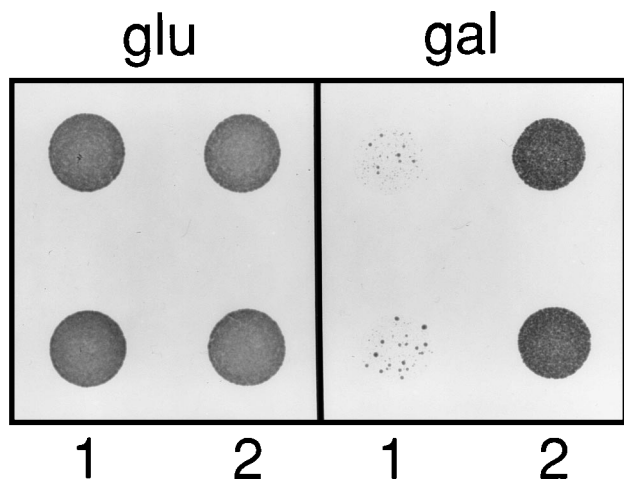


FIG. 5. Effects of *AKR1* on the growth of cells that overexpress *STE4*. Shown is growth on glucose (glu) and galactose (gal) medium of *pGAL-STE4* strain 378 carrying empty vector YEp24 (lane 1) or *AKR1*-bearing, high-copy-number plasmid pPB723 (lane 2). Overnight cultures grown in SC-Ura were diluted 1:30 in water, and 15- μ l aliquots of the diluted cell suspensions were spotted onto YPD (glu) and YPGalRaf (gal) and incubated at 30°C for 28 h (glu) or 46 h (gal). In each case, cultures from two independent transformants were used.

is required for efficient pheromone signaling. To explore this point further, we asked whether *bem1* mutants displayed decreased sensitivity to pheromone in the pheromone arrest halo assay. In this assay, a filter disk containing α -factor is added to a freshly plated lawn of cells. The growth-arresting effect of α -factor later results in a cleared area of no growth in the lawn near the disk. As shown in Fig. 6, whereas deletion of *AKR1* led to a slight increase in the sizes of the halos, deletion of *BEM1* had the opposite effect. From these data, we conclude that Bem1p does indeed facilitate pheromone signaling.

DISCUSSION

Overexpression of Akr1p can suppress the lethality caused by constitutive activation (e.g., because of loss of G_{α} or overexpression of $G_{\beta\gamma}$) of the pheromone response pathway, suggesting that Akr1p can inhibit pheromone signaling. The findings that a partial-loss-of-function allele of *gpa1* becomes lethal in the absence of *AKR1*, that loss of *AKR1* leads to increased expression of pheromone-inducible gene *FUS1*, and that *akr1* mutants display increased sensitivity to the growth-arresting

TABLE 7. Effects of *AKR1* and *BEM1* on the expression of *pFUS1-lacZ*

Strain	Plasmid	β -Galactosidase activity ^a
Y1030 (<i>akr1-Δ1::ura3</i>)	pRS315 (empty, low copy)	31 \pm 7
	pPB741 (<i>AKR1</i> , low copy)	7.4 \pm 0.7
	pPB672 (<i>AKR1</i> , high copy)	4.0 \pm 0.4
Y1036 (<i>akr1-Δ1::ura3</i>)	pRS315 (empty, low copy)	28 \pm 8
	pPB741 (<i>AKR1</i> , low copy)	7.6 \pm 2.9
	pPB672 (<i>AKR1</i> , high copy)	2.9 \pm 0.8
Y1008 (<i>bem1::LEU2</i>)	pRS316 (empty, low copy)	0.6 \pm 0.1
	pCY361 (<i>BEM1</i> , low copy)	3.0 \pm 0.5
Y1029 (<i>bem1::LEU2</i>)	pRS316 (empty, low copy)	0.8 \pm 0.4
	pCY361 (<i>BEM1</i> , low copy)	5.2 \pm 1.6

^a β -Galactosidase activities are given as the means \pm the standard deviations for values derived from five or six independent transformants for Y1036 and Y1030 and from eight independent transformants for Y1029 and Y1008.

TABLE 8. Effects of *AKR1* on the α -factor-induced level of expression of *pFUS1-lacZ*

Plasmid	β -Galactosidase activity ^a		
	0 h	2 h	4 h
YCp50 (empty vector)	30	94	1.5 \times 10 ²
pPB665 (<i>AKR1</i> , low copy)	8.0	88	1.5 \times 10 ²

^a β -Galactosidase activities are given as the average values derived from three or four independent transformants of Y1056 (*pFUS1-lacZ akr1- Δ 1-ura3 bar1::LEU2*) prior to the addition of α -factor (0 h) and 2 and 4 h after the addition of α -factor to 0.02 μ g/ml. All measured values were within 10% of the averages.

activity of α -factor suggest that Akr1p at normal dosage inhibits the pheromone response pathway.

Deletion of *BEM1* leads to decreased expression of *FUS1* and to decreased sensitivity to the growth-arresting effects of pheromone, suggesting that Bem1p, in contrast to Akr1p, promotes pheromone signaling. Given that Bem1p binds to Cdc24p and that Cdc24p and Cdc42p are required for efficient pheromone signaling, it seems likely to us that Bem1p plays a role in the assembly or activation of a $G_{\beta\gamma}$ -responsive signaling complex containing Cdc42p.

Akr1p and Bem1p appear to play only modest roles in pheromone signaling, and cells from which either gene has been deleted mate well (unpublished observations). In contrast, deletion of *AKR1* or *BEM1* has severe effects on cell morphology

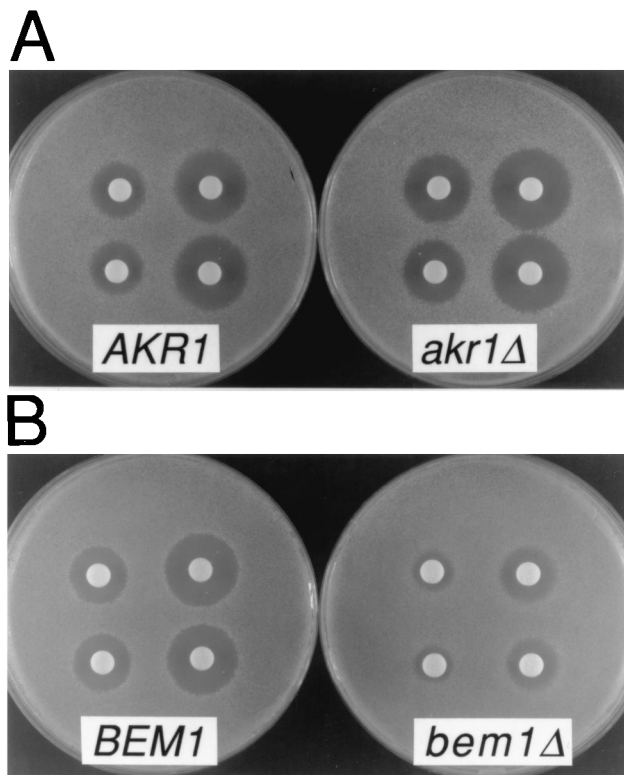


FIG. 6. Effects of *akr1* and *bem1* on the sensitivity to pheromone-induced growth arrest. Filter disks containing 0.15 μ g (left side of each petri plate) or 0.30 μ g (right side of each plate) of α -factor were spotted in duplicate (A) onto lawns of *akr1 bar1* strain Y1026 containing *AKR1*-bearing plasmid pPB741 (*AKR1*) or empty plasmid pRS315 (*akr1 Δ*) or (B) onto lawns of *bem1 bar1* strain Y1031 containing *BEM1*-bearing plasmid pCY361 (*BEM1*) or empty vector pRS316 (*bem1 Δ*).

and viability. These effects occur even in a/α diploids, which cannot respond to pheromone, suggesting that Akr1p and Bem1p play important roles in cellular morphogenesis that are distinct from their roles in pheromone signaling. In some strains, loss of *BEM1* causes cells to become large, round, and multinucleate (4, 9, 10). These phenotypes, combined with physical and genetic interactions linking Bem1p to Cdc24p (28) and Cdc42p (25b), suggest that Bem1p functions with Cdc24p and Cdc42p in bud emergence. Deletion of *AKR1* causes cells to become elongated and to display apparent cytokinesis defects. Although these phenotypes do not resemble the bud emergence defects of *bem1*, *cdc24*, and *cdc42* mutants, they do resemble those defects caused by loss of Cla4p, which is a putative target of Cdc42p.

A model that accommodates both Akr1p's effects on pheromone signaling and the morphological defects of *akr1* mutants is one in which Akr1p promotes the formation or activation of Cdc42p-bearing signaling complexes that contain Cla4p or other targets to the exclusion of those that contain Ste20p. If Cla4p competes with Ste20p for binding to Cdc42p, then loss of *AKR1* could result in both diminished signaling involving Cla4p and increased signaling involving Ste20p.

The identification of Ste4p (G_{β}) during a screen for proteins that displayed two-hybrid interactions with Akr1p raises the possibility that the binding of Ste4p to Akr1p plays a role in pheromone signaling. Although other two-hybrid interactions involving Akr1p (e.g., with Gcs1p) were readily detected in both haploids and a/α diploids, we failed to detect a two-hybrid interaction between Akr1p and Ste4p in a/α cells (unpublished data), raising the possibility that G_{γ} , which is not expressed in a/α diploids (42), may be required for the interaction between Ste4p and Akr1p.

We imagine two possible roles for the potential interaction between Akr1p and $G_{\beta\gamma}$. One possibility is that Akr1p merely acts to antagonize the ability of $G_{\beta\gamma}$ to promote the formation of a functional signaling complex containing Cdc42p, Ste20p, and Ste11p (Fig. 1). Alternatively, Akr1p could itself be one of the targets of $G_{\beta\gamma}$, and the binding of $G_{\beta\gamma}$ to Akr1p might, for example, prevent Akr1p from inhibiting the formation of a functional signaling complex containing Cdc42p, Ste20p, and Ste11p. In future studies, we will investigate whether Akr1p affects the ability of Cdc42p to discriminate among its different potential targets.

ACKNOWLEDGMENTS

We are grateful to Aria Ibrahim and Lei Tang for collecting Sect⁻ mutants; Kendall Blumer, Charlie Boone, Elaine Elion, Scott Givan, Lee Hartwell, Duane Jenness, James Konopka, Peter Pryciak, George F. Sprague, Jr., David Stone, and Malcolm Whiteway for very helpful advice and discussions; Steve Elledge for the two-hybrid library; and Charlie Boone, David Stone, James Konopka, Joe Horecka, George F. Sprague, Jr., Karen Clark, Malcolm Whiteway, and Rolf Sternglanz for plasmids and strains.

This work was supported by a National Institutes of Health grant (GM46271) and a Searle Scholar award to A. Bender and by a postdoctoral fellowship from the Walther Cancer Institute to J. Peterson.

REFERENCES

- Adams, A. E. M., D. I. Johnson, R. M. Longnecker, B. F. Sloat, and J. R. Pringle. 1990. *CDC42* and *CDC43*, two additional genes involved in budding and the establishment of cell polarity in the yeast *Saccharomyces cerevisiae*. *J. Cell Biol.* **111**:131-142.
- Bartel, P., C.-T. Chien, R. Sternglanz, and S. Fields. 1993. Using the two-hybrid system to detect protein-protein interactions, p. 153-179. In D. A. Hartley (ed.), *Cellular interactions in development: a practical approach*. Oxford University Press, Oxford.
- Bender, A., and J. R. Pringle. 1989. Multicopy suppression of the *cdc24* budding defect in yeast by *CDC42* and three newly identified genes including the *ras*-related gene *RSR1*. *Proc. Natl. Acad. Sci. USA* **86**:9976-9980.
- Bender, A., and J. R. Pringle. 1991. Use of a screen for synthetic lethal and multicopy suppressor mutants to identify two new genes involved in morphogenesis in *Saccharomyces cerevisiae*. *Mol. Cell. Biol.* **11**:1295-1305.
- Bender, A., and G. F. Sprague, Jr. 1989. Pheromones and pheromone receptors are the primary determinants of mating specificity in the yeast *Saccharomyces cerevisiae*. *Genetics* **121**:463-476.
- Bender, L., H. S. Lo, H. Lee, V. Kokojan, J. Peterson, and A. Bender. Associations among PH and SH3 domain-containing proteins and Rho-type GTPases in yeast. Submitted for publication.
- Botstein, D., S. C. Falco, S. E. Stewart, M. Brennan, S. Scherer, D. T. Stinchcomb, K. Struhl, and R. W. Davis. 1979. Sterile host yeasts (SHY): a eukaryotic system of biological containment for recombinant DNA experiments. *Gene* **8**:17-24.
- Carlson, M., and D. Botstein. 1982. Two differentially regulated mRNAs with different 5' ends encode secreted and intracellular forms of yeast invertase. *Cell* **28**:145-154.
- Chant, J., K. Corrado, J. R. Pringle, and I. Herskowitz. 1991. Yeast *BUD5*, encoding a putative GDP-GTP exchange factor, is necessary for bud site selection and interacts with bud formation gene *BEM1*. *Cell* **65**:1213-1224.
- Chenevert, J., K. Corrado, A. Bender, J. Pringle, and I. Herskowitz. 1992. A yeast gene (*BEM1*) necessary for cell polarization whose product contains two SH3 domains. *Nature (London)* **356**:77-79.
- Chenevert, J., N. Valtz, and I. Herskowitz. 1994. Identification of genes required for normal pheromone-induced cell polarization in *Saccharomyces cerevisiae*. *Genetics* **136**:1287-1297.
- Chien, C., and R. Sternglanz. Personal communication.
- Choi, K.-Y., B. Satterberg, D. M. Lyons, and E. A. Elion. 1994. Ste5 tethers multiple protein kinases in the MAP kinase cascade required for mating in *S. cerevisiae*. *Cell* **78**:499-512.
- Clark, K. L., D. Dignard, D. Y. Thomas, and M. Whiteway. 1993. Interactions among the subunits of the G protein involved in *Saccharomyces cerevisiae* mating. *Mol. Cell. Biol.* **13**:1-8.
- Cvrčková, F., C. De Virgilio, E. Manser, J. R. Pringle, and K. Nasmyth. 1995. Ste20-like protein kinases are required for normal localization of cell growth and for cytokinesis in budding yeast. *Genes Dev.* **9**:1817-1830.
- Cvrčková, F., and K. Nasmyth. 1993. Yeast G_1 cyclins *CLN1* and *CLN2* and a GAP-like protein have a role in bud formation. *EMBO J.* **12**:5277-5286.
- Hagen, D. C., G. McCaffrey, and G. F. Sprague, Jr. 1986. Evidence the yeast *STE3* gene encodes a receptor for the peptide pheromone a factor: gene sequence and implications for the structure of the presumed receptor. *Proc. Natl. Acad. Sci. USA* **83**:1418-1422.
- Harper, J. W., G. R. Adami, N. Wei, K. Keyomarsi, and S. J. Elledge. 1993. The p21 Cdk-interacting protein Cip1 is a potent inhibitor of G1 cyclin-dependent kinases. *Cell* **75**:805-816.
- Hartwell, L. H., R. K. Mortimer, J. Culotti, and M. Culotti. 1973. Genetic control of the cell division cycle in yeast. V. Genetic analysis of *cdc* mutants. *Genetics* **74**:267-286.
- Ireland, L. S., G. C. Johnston, M. A. Drebort, N. Dhillon, A. J. DeMaggio, M. F. Hoekstra, and R. A. Singer. 1994. A member of a novel family of yeast 'Zn-finger' proteins mediates the transition from stationary phase to cell proliferation. *EMBO J.* **13**:3812-3821.
- Kidd, S. 1992. Characterization of the *Drosophila cactus* locus and analysis of interactions between cactus and dorsal proteins. *Cell* **71**:623-635.
- Koshland, D., J. C. Kent, and L. H. Hartwell. 1985. Genetic analysis of the mitotic transmission of minichromosomes. *Cell* **40**:393-403.
- Leberer, E., D. Dignard, D. Harscus, D. Y. Thomas, and M. Whiteway. 1992. The protein kinase homologue Ste20p is required to link the yeast pheromone response G-protein $\beta\gamma$ subunits to downstream signalling components. *EMBO J.* **11**:4815-4824.
- Liu, H., C. A. Styles, and G. R. Fink. 1993. Elements of the yeast pheromone response pathway required for filamentous growth of diploids. *Science* **262**:1741-1744.
- Lux, S. E., K. M. John, and V. Bennett. 1990. Analysis of cDNA for human erythrocyte ankyrin indicates a repeated structure with homology to tissue-differentiation and cell-cycle control proteins. *Nature (London)* **344**:36-42.
- Ma, H., S. Kunes, P. J. Schatz, and D. Botstein. 1987. Plasmid construction by homologous recombination in yeast. *Gene* **58**:201-216.
- Mack, D., and A. Bender. Unpublished data.
- Mack, D., H. S. Lo, and A. Bender. Unpublished data.
- Michaely, P., and V. Bennett. 1992. The ANK repeat: a ubiquitous motif involved in macromolecular recognition. *Trends Cell Biol.* **2**:127-129.
- Miyajima, I., M. Nakafuku, N. Nakayama, C. Brenner, A. Miyajima, K. Kaibuchi, K. Arai, Y. Kaziro, and K. Matsumoto. 1987. *GPA1*, a haploid-specific essential gene, encodes a yeast homolog of mammalian G protein which may be involved in mating factor signal transduction. *Cell* **50**:1011-1019.
- Peterson, J., Y. Zheng, L. Bender, A. Myers, R. Cerione, and A. Bender. 1994. Interactions between the bud emergence proteins Bem1p and Bem2p and Rho-type GTPases in yeast. *J. Cell Biol.* **127**:1395-1406.
- Pringle, J. R., R. A. Preston, A. E. M. Adams, T. Stearns, D. G. Drubin, B. K. Haarer, and E. W. Jones. 1989. Fluorescence microscopy methods for yeast.

- Methods Cell Biol. **31**:357–435.
30. **Printen, J. A., and G. F. Sprague, Jr.** 1994. Protein-protein interactions in the yeast pheromone response pathway: Ste5p interacts with all members of the MAP kinase cascade. *Genetics* **138**:609–619.
 31. **Ramer, S. W., and R. W. Davis.** 1993. A dominant truncation allele identifies a gene, *STE20*, that encodes a putative protein kinase necessary for mating in *Saccharomyces cerevisiae*. *Proc. Natl. Acad. Sci. USA* **90**:452–456.
 32. **Reynolds, A., and V. Lundblad.** 1989. Yeast vectors and assays for expression of cloned genes, p. 13.6.1–13.6.4. *In* F. M. Ausubel, R. Brent, R. E. Kingston, D. D. Moore, J. G. Seidman, J. A. Smith, and K. Struhl (ed.), *Current protocols*. John Wiley and Sons, New York.
 33. **Rose, M. D., P. Novick, J. H. Thomas, D. Botstein, and G. R. Fink.** 1987. A *Saccharomyces cerevisiae* genomic plasmid bank based on a centromere-containing shuttle vector. *Gene* **60**:237–243.
 34. **Schneider, K. R., R. L. Smith, and E. K. O'Shea.** 1994. Phosphate-regulated inactivation of the kinase PHO80-PHO85 by the CDK inhibitor PHO81. *Science* **266**:122–126.
 35. **Serrano, M., G. J. Hannon, and D. Beach.** 1993. A new regulatory motif in cell-cycle control causing specific inhibition of cyclin D/CDK4. *Nature (London)* **366**:704–707.
 36. **Sikorski, R. S., and P. Hieter.** 1989. A system of shuttle vectors and yeast host strains designed for efficient manipulation of DNA in *Saccharomyces cerevisiae*. *Genetics* **122**:19–27.
 37. **Simon, M.-N., C. De Virgilio, B. Souza, J. R. Pringle, A. Abo, and S. I. Reed.** 1995. Role for the Rho-family GTPase Cdc42 in yeast mating-pheromone signal pathway. *Nature (London)* **376**:702–705.
 38. **Sprague, G. F., Jr., and J. W. Thorner.** 1992. Pheromone response and signal transduction during the mating process of *Saccharomyces cerevisiae*, p. 657–744. *In* E. W. Jones, J. R. Pringle, and J. R. Broach (ed.), *The molecular and cellular biology of the yeast Saccharomyces: gene expression*, vol. 2. Cold Spring Harbor Laboratory Press, Cold Spring Harbor, N.Y.
 39. **Stevenson, B. J., N. Rhodes, B. Errede, and G. F. Sprague, Jr.** 1992. Constitutive mutants of the protein kinase STE11 activate the yeast pheromone response pathway in the absence of the G protein. *Genes Dev.* **6**:1293–1304.
 40. **Vojtek, A. B., S. M. Hollenberg, and J. A. Cooper.** 1993. Mammalian Ras interacts directly with the serine/threonine kinase Raf. *Cell* **74**:205–214.
 41. **Wharton, K. A., K. M. Johansen, T. Xu, and S. Artavanis-Tsakonas.** 1985. Nucleotide sequence from the neurogenic locus *notch* implies a gene product that shares homology with proteins containing EGF-like repeats. *Cell* **43**:567–581.
 42. **Whiteway, M., L. Hougan, D. Dignard, D. Y. Thomas, L. Bell, G. C. Saari, F. J. Grant, P. O'Hara, and V. L. MacKay.** 1989. The *STE4* and *STE18* genes of yeast encode potential β and γ subunits of the mating factor receptor-coupled G protein. *Cell* **56**:467–477.
 43. **Whiteway, M. S., C. Wu, T. Leeuw, K. Clark, A. Fourest-Lieuvain, D. Y. Thomas, and E. Leberer.** 1995. Association of the yeast pheromone response G protein $\beta\gamma$ subunits with the MAP kinase scaffold Ste5p. *Science* **269**:1572–1575.
 44. **Wu, C., M. Whiteway, D. Y. Thomas, and E. Leberer.** 1995. Molecular characterization of Ste20p, a potential mitogen-activated protein or extracellular signal-regulated kinase (MEK) kinase from *Saccharomyces cerevisiae*. *J. Biol. Chem.* **270**:15984–15992.
 45. **Zhao, Z.-S., T. Leung, E. Manser, and L. Lim.** 1995. Pheromone signalling in *Saccharomyces cerevisiae* requires the small GTP-binding protein Cdc42p and its activator *CDC24*. *Mol. Cell. Biol.* **15**:5246–5257.
 46. **Zheng, Y., R. Cerione, and A. Bender.** 1994. Control of the yeast bud-site assembly GTPase Cdc42: catalysis of guanine nucleotide exchange by Cdc24 and stimulation of GTPase activity by Bem3. *J. Biol. Chem.* **269**:2369–2372.